ORIGINAL PAPER

G. Taucher-Scholz · J. Heilmann · M. Schneider · G. Kraft

Detection of heavy-ion-induced DNA double-strand breaks using static-field gel electrophoresis

Abstract Radiation-induced DNA double-strand breaks (DSBs) were measured in Chinese hamster ovary cells (CHO-K1) using an experimental protocol involving static-field gel electrophoresis following exposure to various accelerated ions. Dose-effect curves were set up, and relative biological efficiencies (RBEs) for DSB induction were determined for different radiation qualities. RBEs around 1 were obtained for low energy deuterons (6–7 keV/μm), while for high energy oxygen ions (20 keV/μm) an RBE value slightly greater than 1 was determined. Low energetic oxygen ions (LET ≈ 250 keV/μm) were found to show RBEs substantially below unity, and for higher LET particles (≥250 keV/μm) RBEs for DSB induction were generally found to be smaller than 1. The data presented here are in line with the generally accepted view that not induced DSBs, but rather misrepaired or unrepaired DNA lesions are related to cellular inactivation.

Introduction

In living cells, DNA is the most radiosensitive biomolecule (Cole et al. 1975). Typical DNA lesions include single-strand breaks (SSBs), double-strand breaks (DSBs) or cross-links. The dominant lesions responsible for cell death are DSBs. Cell killing is thought to be the result of residual unrepaired DSBs (Frankenberg et al. 1981; Bryant 1985; Wlodek and Hittelman 1988).

The interaction of accelerated heavy ions with matter is similar to other ionizing radiations. Electron-ion pairs are created, either in the target molecules or in the surrounding water, resulting in reactive radicals. The spatial distribution of the energy depositing events is restricted to the particle track. The classical radiobiological parameter to characterize radiations of different ionizing potential is the linear energy transfer [LET (keV/μm)] (Zirkle and Tobias 1953).

To describe the effects of different ionizing radiations on cellular DNA, both measurements on DSB induction and DNA rejoining are necessary. The latter phenomenological approach gives information on the extent and kinetics of cellular DNA damage processing, while induction data allow the calculation of the relative biological effectiveness (RBE). Data on both molecular and cellular effects of heavy ions are essential to provide a radiobiological basis for therapy planning.

Only a few publications deal with DNA-DSB induction in mammalian cells following particle irradiation (Kampf and Eichhorn 1983; Heilmann et al. 1993; Weber and Flentje 1993). For cellular inactivation, an RBE maximum at LET values around 100 keV/μm is well documented (Barendsen et al. 1963). Concerning DSB induction, only data from Kampf and co-workers cover this LET region. The other publications deal with heavy particles ($Z \geq 10$) at low energies. For light ions ($Z \leq 10$) there are almost no data available in the low LET regime. However, these data, together with results from survival experiments, provide the input necessary for radiobiological modelling.

Several different experimental protocols have been established for the detection of heavy-ion-induced DSBs: ultracentrifugation in neutral sucrose gradients, neutral filter elution and pulsed-field gel electrophoresis (PFGE). While the first two methods have been well known for many years, PFGE was introduced for DSB measurements in 1989 (Blöcher et al. 1989). Since then, many varying experimental protocols have been described in the literature. Recent publications have reported similar results with either PFGE or gel electrophoresis in a static electric field (SFGE) (Wlodek et al. 1991; Schneider et al. 1994), as DNA fragments need not be separated by size in this application.

We developed a procedure for DNA-DSB detection involving SFGE and densitometric scanning of photographic negatives from ethidium-bromide-stained gels. The high selectiveness of the assay for DSBs was demonstrated with DNaseI treatment, and a standardized calibration procedure resulted in almost perfect agreement with experiments using radiolabelled cells after heavy-ion irradiation

G. Taucher-Scholz (✉) · J. Heilmann · M. Schneider · G. Kraft
GSI Darmstadt, Postfach 110552, D-64220 Darmstadt, Germany

(Schneider et al. 1994). This assay was applied to measure the induction and rejoining of DNA-DSBs in Chinese hamster ovary (CHO-K1) cells after irradiation with different heavy ions (D, C, O, Ne, Ar, Xe, Pb) of specific energies between 3 MeV/u and 500 MeV/u (MeV/u: energy/nucleon).

Materials and methods

Cells and cell culture

CHO-K1 obtained from the American Type Culture Collection were grown in culture flasks (Greiner) as monolayers using Hams F12 medium (Boehringer) supplemented with 10% fetal bovine serum and 2 mmol/l glutamine. Incubator settings were 37 °C and 5% CO_2. Exponential growth was maintained by regular passaging of the cells.

Preparation of cells for irradiation

Late log-phase cells were used in all irradiation experiments. For X-rays and high-energy particles, irradiation was carried out in agarose plugs. Cells were harvested from 75-cm^2 culture flasks at a density of about $6-9\times10^4$ cells/cm^2. After determination of the cell number in a cell counter (Coulter Electronics), cells were embedded in 0.5% low melting point agarose (Sigma, Type VII), and the suspension was poured into plug moulds before irradiation. The final cell number in the agarose plugs was 2.5×10^6 cells/ml. Until irradiation, plugs were stored on ice in phosphate-buffered saline (PBS; Gibco).

The limiting particle range of accelerated heavy ions with energies below 15 MeV/u called for irradiation of the cells as monolayers. In this case, cells were grown to a density of about 6×10^4 cells/cm^2 in small petri dishes (35 mm, Greiner) and irradiated directly as described below.

Irradiation

X-ray samples were irradiated using a Siemens Stabiliplan X-ray generator (type TR 300F) operated at 250 kV and 20 mA, filtered with 1 mm of aluminium and 1 mm of copper at a dose rate of 7 Gy/min. Dosimetry was performed with a DL4 dosimeter (PTW) calibrated by the Fricke method. Accelerated heavy ions were provided by the accelerators at Gesellschaft für Schwerionenforschung (GSI), Darmstadt.

Low-energy ions below 15 MeV/u were generated with the UNILAC linear accelerator. Homogenous irradiation was achieved using a defocused beam and ensuring excentric movement of the sample. The particle fluence was measured via a secondary electron monitor. Calibration was achieved by microscopic counting of etched particle tracks in glass or plastic. The irradiation facility has been described in detail elsewhere (Kraft et al. 1980).

For higher particle energies (397 MeV/u oxygen and 482 MeV/u lead) the heavy ion synchrotron (SIS) was used. Here, homogeneity within the irradiated area was ensured using a raster scanning technique. As with the UNILAC, dosimetry relied on a secondary electron monitor and microscopic counting of particle tracks. A comprehensive description of the irradiation technique is given by Haberer and co-workers (1993).

Cell lysis and incubation for rejoining

After irradiation, cells were either lysed directly or kept under culture conditions for different time intervals to allow strand-break rejoining. For post-irradiation incubation, petri dishes irradiated at the UNILAC were filled with prewarmed medium and placed in an in-cubator. Cells irradiated in agarose plugs were transferred into medium-filled petri dishes and incubated at 37 °C, too.

Cells irradiated in monolayers had to be embedded in agarose for further treatment. Residual medium was removed by washing twice with PBS. Cell scrapers (Greiner) were used to remove the monolayer from the culture dishes. Cells from three dishes were pooled, resuspended in PBS, and embedded in agarose plugs at a density of 2.5×10^6 cells/ml as already described. All steps were performed on ice to minimize repair during preparation.

Cells in the agarose plugs were incubated in lysis buffer (0.5 mol/l EDTA, 2% sodium lauryl sarcosinate) containing 1 mg/ml proteinase K (Boehringer). They were stored at 0 °C for 1 h to guarantee diffusion of the enzyme into the agarose before lysis. Protein digests were performed at 50 °C for 20 h. Afterwards, plugs were equilibrated in TE buffer (10 mmol/l TRIS, 1 mmol/l EDTA, pH 8) and used directly for electrophoresis.

Static-field gel electrophoresis

Plug pieces equilibrated in TE buffer were loaded on 0.5% agarose gels (Biorad Ultrapure DNA grade agarose) and subjected to electrophoresis at a field strength of 1.85 V/cm in 0.5 TBE buffer (45 mmol/l TRIS, 45 mmol/l boric acid, 2 mmol/l EDTA) for 16 h. Gels were stained for at least 3 h with ethidium bromide (2 μg/ml) and destained overnight at 4 °C in distilled water. They were photographed on an UV transilluminator with an orange filter using Polaroid 55 film. Exposure was optimized to achieve a linear proportional increase of film blackening with the intensity of fluorescence from the DNA.

Densitometric scanning

The procedure has been described in detail elsewhere (Schneider et al. 1994). Briefly, transilluminated photographic negatives were digitized via a CCD camera and a frame grabber. Images with a resolution of 512×512 pixels and 8-bit colour were analysed with a computer program. A linear background was subtracted for calculation. Yields of released DNA obtained from the negatives were determined. Standardization was achieved in X-ray experiments by measuring in parallel both the amount of DNA eluted via densitometry and the fraction of DNA retained in the well as isotope activity. A calibration curve was then set up and used to calculate the fraction of DNA retained from the densitometric data obtained in heavy ion experiments. The applicability of this procedure has been tested using heavy-ion-irradiated, radiolabelled cells (Schneider et al. 1994).

Results

DNA DSB induction was investigated following exposure of CHO-K1 cells to deuterium, oxygen, argon, xenon and lead ions. From the densitometric analysis of the different electrophoresis runs, dose-effect curves were prepared (Fig. 1). Due to the limited accessibility of the accelerators, experiments with heavy ions were only performed once, so error bars cannot be given. However, taking together fluctuations of dosimetry and deviations within the experimental procedure, errors are likely to be below 20%.

The physical parameters of the heavy ions used are given in Table 1. To calculate the physical dose from a given particle fluence, the following equation was used:

$$\text{Dose [Gy]} = 1.602\times10^{-9}\times\text{LET [keV/μm]}$$
$$\times \text{fluence [p/cm}^2] \times 1/\rho \text{ [g/cm}^3]$$

Fig. 1 Double-strand break (DSB) induction in CHO-K1 cells as measured with static-field gel electrophoresis after (a) X-irradiation or treatment with (b) 7.1 MeV/u deuterium, (c) 400 MeV/u oxygen or (d) 500 MeV/u lead ions. Plotted is the fraction of DNA retained as a function of dose or particle fluence. Efficiency of DSB induction per particle increases with increasing atomic number (b–d)
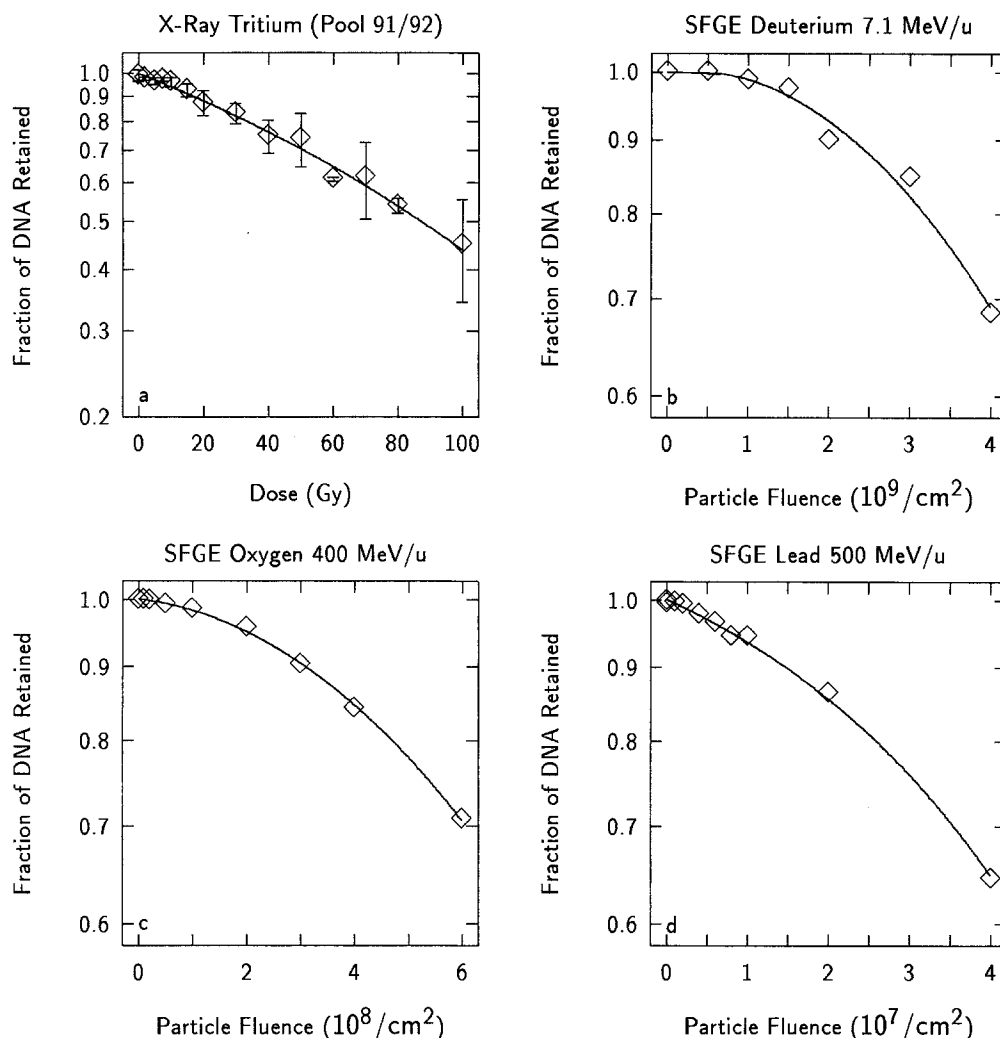

Table 1 Physical data on the particle beams used and relative biological efficiency (RBE) values for DSB induction

Ion	Energy (MeV/u)	LET (keV/μm)	$D_{0.7}$ (Gy)	$RBE_{0.7}$
X-ray	–	2	51.0	1.0
D	2.9	12	102.0	0.5
	6.1	6.6	31.6	1.61
	7.1	6	37.9	1.35
O	11.4	250	134.0	0.38
	397.0	20	19.5	2.6
Ar	5.3	1734	106.0	0.48
	13.3	1047	73.0	0.7
Xe	9.1	7990	650.0	0.08
	11.8	7390	230.0	0.22
Pb	482.0	1660	93.0	0.55

LET, linear energy transfer

where LET is the linear energy transfer at the particles' energy and ρ is the buoyant density of the target material (usually 1 g/cm³ for biological samples).

Dose-effect curves all have a curvilinear shape with an initial shoulder, despite the linear induction of DSB with dose (Ward 1990). The difference between the exclusion size of the gel and the size of a hamster chromosome (6 Mbp vs 100 Mbp) is responsible for the shape of the induction curves (Blöcher 1990). Chromosome fragments larger than 6 Mbp will not enter the gel, and hence, the DNA damage induced at low doses is underestimated, resulting in a shoulder. The shape of effect curves up to an ordinate value of about 0.5 fraction of DNA retained has proven to be almost independent of the quality of the radiation used (Fig. 1). Therefore, RBE values calculated for different fractions of DNA retained are almost identical. We chose a fraction of 0.7 of DNA retained as the reference point for RBE calculation, as the induction response is almost linear here and experimental errors are low due to high-intensity signals in the densitometry of the photographic films. The particle fluence corresponding to this level of DNA damage was calculated and converted into a physical dose as described above. The relative biological efficiency is given by:

$$RBE = \frac{dose_{0.7(X-ray)}}{dose_{0.7(particle\ radiation)}}$$

The calculated RBE values are compiled in Table 1.

A flattening of the dose response at X-ray doses larger than about 100 Gy was observed for the experimental set-up applied here (Schneider et al. 1994). In many investigations dealing with the detection of intracellularly induced DSBs via electrophoresis, a similar effect has been reported (Ager et al. 1990; Stamato and Denko 1990). For this methodological reason, DSB yields cannot be inferred from the final slope of the dose-effects curves.

Results of rejoining experiments with X-rays, Ne and Xe ions are compiled in Fig. 2. Rejoining with high energetic Ne ions is fast, taking into account that RBE≈1 and hence the damage induced initially by 38 Gy Ne ions is about two times higher than for 20 Gy X-rays. With 10 MeV/u Ne ions, rejoining is impaired, especially when regarding the level of residual damage after 3 h incubation. After irradiation with Xe ions, incubation for rejoining has only a minor effect, with 80% of the initial damage remaining after 3 h.

Fig. 2 Rejoining of DNA-DSB after irradiation with (**a**) 20 Gy X-rays (◇), (**b**) 38 Gy 390 MeV/u Ne ions (□), (**c**) 13 Gy 10 MeV/u NE ions (+), and (**d**) 77 Gy 9.1 MeV/u Xe ions (×). Linear energy transfers (LETs) correspond to 2 keV/μm, 30 keV/μm, 370 keV/μm and 7990 keV/μm, respectively. Curves were all fitted by eye

Discussion

In addition to classical methods like neutral sucrose sedimentation and neutral filter elution to detect DNA DSBs in mammalian cells, a variety of experimental protocols have evolved including different forms of agarose gel electrophoresis, the comet assay and the precipitation assay (-Olive 1988; Blöcher et al. 1989; Ager and Dewey 1990; Stamato and Denko 1990; Olive et al. 1992). The electrophoretic methods have clear advantages as they offer simplicity, speed, sensitivity and a clear theoretical basis all in one. In our experimental set-up, the densitometric analysis of the blackening of photographic negatives was calibrated with results obtained with radiolabelled cells after X-irradiation (Schneider et al. 1994). This procedure allowed us to drop radiolabelling in the accelerator experiments, which was limited by strict safety regulation.

Despite all known differences and obstacles of the different detection methods, it has been proven that results obtained with either sedimentation or neutral filter elution or gel electrophoresis of cellular DNA are very much the same (Iliakis et al. 1991). To compare our data with results obtained by other groups using these techniques, the RBE serves as the most convenient and reliable parameter. Figure 3 gives a compilation of RBE data for both low and high LET particle radiations.

Concerning low LET particles, most data on the intracellular induction of DNA-DSBs were collected with proton and α-particle beams. In the LET range up to 60 keV/μm, the published RBE values vary from 0.5 to 1.6. While the data set reported by Kampf shows a flat but steady increase in RBE (Kampf 1983), proton and α-particle data investigated by two groups independently lie close together, with RBE values between 0.7 and 1.0 (Prise et al. 1990; Goodhead et al. 1992). RBEs found by us for deuterons were about 1.5 for 6 keV/μm and 6.6 keV/μm particles, while it was only 0.5 for deuterons with a LET of 12 keV/μm. The first two values are well within the trend
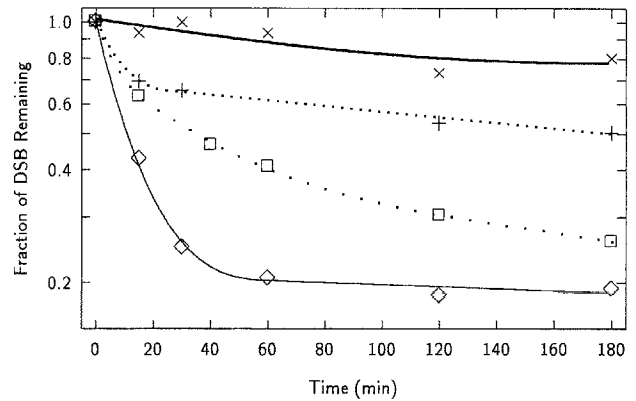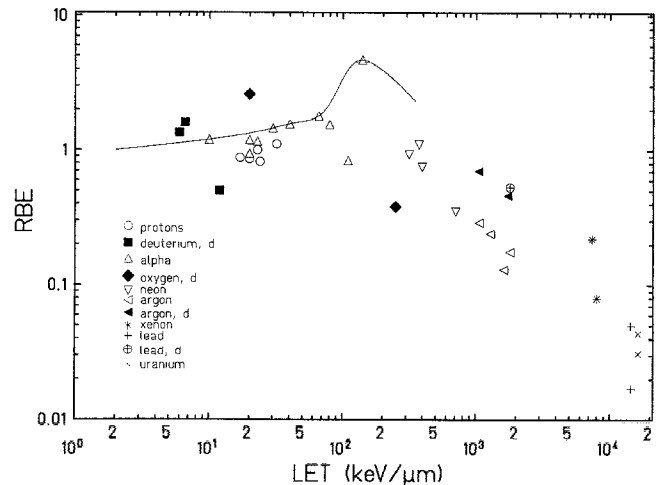

Fig. 3 Relative biological efficiency for the intracellular induction of DNA DSB. The *fitted line* corresponds to data from Kampf and Eichhorn (1983), the α and proton data in the LET region from 17 keV/μm to 110 keV/μm are from Jenner et al. (1992) and Prise et al. (1990), while high LET data were taken from Weber and Flentje (1993) and Heilmann et al. (1993). Except for the latter data set, in which non-permanent human skin fibroblast cell lines were used, all other experiments were performed with V79 cells. Our data (CHO-K1) are represented by *filled symbols* and are labelled with *d* in the key

seen in the literature, while the last is quite low. It is unlikely that an increase in LET in this regime of low energetic particles with low ionization densities results in a sharp decline of RBE. Therefore, we believe that an RBE around unity is most realistic for light ions and LET values up to about 60 keV/μm.

Quite unexpectedly, a RBE of 2.6 was determined for a high-energetic oxygen beam (400 MeV/u, 20 keV/μm). This value is higher than published data for protons and α-particles in this LET region (see Fig. 3). It should be kept

in mind that the RBE constitutes a quotient of data with a systematic error of around 20%. Therefore, considerable scatter of these values cannot be avoided. However, in an independent experiment using a slightly modified protocol for DSB evaluation (manuscript in preparation), a RBE of 1.9 was obtained for the 400 MeV/u oxygen particles. RBE values higher than unity cannot be ruled out.

In this context, the production of clustered ionization events should be discussed (Brenner and Ward 1992). The interaction of accelerated particles with the target material generates electrons. High-energetic electrons themselves can produce secondary and even higher-order electrons, all of which can lead to the formation of radicals. Thus, in a small target volume, multiple radicals may be produced by one primary ionization event. The resulting lesion within a DNA double strand will be detected as DSB by all assays currently available. Calculations based on the formation of DSBs in so-called locally multiply damaged sites (LMDS; Ward 1985) show an initial increase of RBE at very low LET ($\leq$30 keV/μm), followed by a more or less steady decrease for higher LET values, depending on the size of the volume considered and the number of ionizations assumed within this volume. This theory offers an explantation for high RBE at low LET with a credible physical and chemical background.

Going to higher LET values (100–200 keV/μm), data by Kampf and Eichhorn (1983) with RBE values well above unity are in contrast to measurements with α-particles (110 keV/μm; Prise et al. 1990) and data obtained with oxygen and neon ions (250–400 keV/μm; Heilmann et al. 1993; Weber and Flentje 1993). Our RBE calculation for oxygen at 250 keV/μm shows, in agreement with the latter data sets, a value less than 1.

For LET values beyond 300 keV/μm, RBE values are generally much smaller than 1, declining not only with increasing LET, but also with the Z (atomic number) of the particle. The decline of RBE with LET is most obvious for lead ions, as some RBEs are available from 1800 keV/μm to 14 300 keV/μm. However, the same tendency can be seen for neon and argon ions. This separation in distinct curves is well-known from studies on DSB induction in SV40 viral DNA in dilute solution (Roots et al. 1990). For this experimental system, a comprehensive data set exists, together with theoretical calculations (Katz and Wesely 1991).

The changes in the quality of the lesions induced by different particle radiations can be seen best when looking at rejoining kinetics (Fig. 2). With increasing atomic number and LET, kinetics of DNA DSB rejoining slow down, and the level of damage remaining after 3 h, the maximum incubation time, increases. After irradiation with low-energy Xe ions, only a minute amount of rejoining was detected. This decline in the rejoining capacity of cells for different particle radiations cannot be explained as an effect of damage quantity, but is very much in favour of a change in the quality of the lesions induced. As the fidelity of DNA damage processing is essential for cellular survival, systematic data on DSB induction and rejoining will be collected in the future to gain a clear picture of its systematics. This is

especially necessary as the RBE-LET relationship for DSB production in the region relevant for particle radiotherapy ($\approx$10 up to a few hundred keV/μm) is still unclear. Further experiments with highly energetic light ions will cover this matter in more detail.

References

Ager D, Dewey W (1990) Calibration of pulsed field electrophoresis for measurement of DNA double-strand breaks. Int J Radiat Biol 58:249–259

Ager D, Dewey W, Gardiner K, Harvey W, Johnson R, Waldren C (1990). Measurement of radiation-induced DNA double-strand breaks by pulsed field electrophoresis. Radiat Res 122:181–187

Barendsen G, Walter H, Fowler J, Bewley D (1963) Effects of different ionizing radiations on human cells in tissue culture. Radiat Res 18:106–119

Blöcher D (1990) In CHEF electrophoresis a linear induction DSB corresponds to a nonlinear fraction of extracted DNA with dose. Int J Radiat Biol 57:7–12

Blöcher D, Einspenner M, Zajackowski J (1989) CHEF electrophoresis, a sensitive technique for the determination of DNA double-strand breaks. Int J Radiat Biol 56:437–448

Brenner D, Ward J (1992) Constraints on energy deposition and target size of multiply damaged sites associated with DNA double-strand breaks. Int J Radiat Biol 61:737–748

Bryant P (1985) Enzymatic restriction of mammalian cell DNA: evidence for double-strand breaks as potentially lethal lesions. Int J Radiat Biol 48:55–60

Cole A, Robinson S, Shonka F, Datta R, Chen R (1975) Organization of mammalian chromosomes interpreted from radiation and other studies. Biophys J 13:207–222

Frankenberg D, Frankenberg-Schwager M, Blöcher D, Harbich R (1981) Evidence for DNA double-strand breaks as the critical lesions in yeast cells irradiated with sparsely or densely ionizing radiation under oxic or anoxic conditions. Radiat Res 88:524–532

Goodhead D, Belli M, Mill A, Bance D, Allen l, Hall S, Ianzini F, Simone G, Stevens D, Stretch A, Tabocchini M, Wilkinson R (1992) Direct comparison between protons and alpha particles of the same LET. I. Irradiation methods and inactivation of asynchronous V79, HeLa and C3H 10T$\frac{1}{2}$ cells. Int J Radiat Biol 61:611–624

Haberer T, Becher W, Schardt D, Kraft G (1993). Magnetic scanning system for heavy ion therapy. Nucl Inst Methods A330:296–305

Heilmann J, Rink H, Taucher-Scholz G, Kraft G (1993) DNA strand break induction and rejoining and cellular recovery in mammalian cells after heavy ion irradiation. Radiat Res 135:46–55

Iliakis G, Blöcher D, Metzger L, Pantelias G (1991) Comparison of DNA double-strand break rejoining as measured by pulsed field gel electrophoresis, neutral sucrose gradient centrifugation and nonunwinding filter elution in irradiated plateau-phase CHO cells. Int J Radiat Biol 59:927–939

Jenner T, Belli M, Goodhead D, Ianzini F, Simone G, Tabocchini M (1992) Direct comparison of biological effectiveness of protons and alpha-particles of the same LET. III. Initial yield of DNA double-strand breaks in V79 cells. Int J Radiat Biol 61:631–637

Kampf G (1983) Die Erzeugung von DNS-Strangbrüchen durch ionisierende Strahlen unterschiedlicher Qualität und ihre Bedeutung für die Zellinaktivierung. Technical report, Zentralinstitut für Kernforschung, Rossendorf KfR 504 Habil-Schrift

Kampf G, Eichhorn K (1983) DNA strand breakage by different radiation qualities and relations to cell killing: further results after the influence of α-particles and carbon ions. Stud Biophys 93:17–26

Katz R, Wesely S (1991) Cross sections for single and double strand breaks in SV-40 virus in EO buffer after heavy ion irradiation: experiment and theory. Radiat Environ Biophys 30:81–85

106

Kraft G, Daues H, Fischer B, Kopf U, Liebold H, Quis D, Stelzer H (1980) Irradiation chamber and sample changer for biological samples. Nucl Instr Methods 168:175–179

Olive P (1988) DNA precipitation assay: a rapid and simple method for detecting DNA damage in mammalian cells. Environ Mol Mutagen 11:487–495

Olive P, Wlodek D, Durand R, Banáth J (1992) Factors influencing DNA migration from individual cells subjected to gel electrophoresis. Exp Cell Res 198:259–267

Prise K, Folkard M, Davies S, Michael B (1990) The irradiation of V 79 mammalian cells by protons with energies below 2 MeV. II. Measurement of oxygen enhancement ratios and DNA damage. Int J Radiat Biol 58:261–277

Roots R, Holley W, Chatterjee A, Irizarry M, Kraft G (1990). The formation of strand breaks in DNA after high-LET irradiation: a comparison of data from in vitro and cellular systems. Int J Radiat Biol 58:55–69

Schneider M, Taucher-Scholz G, Heilmann J, Kraft G (1994) Combination of static field gel electrophoresis and densitometric scanning for the determination of radiation induced DNA double-strand breaks in CHO-cells. Radiat Environ Biophys, 33:111–124

Stamato T, Denko N (1990) Asymmetric field inversion gel electrophoresis: a new method for detecting DNA double-strand breaks in mammalian cells. Radiat Res 121:196–205

Ward J (1985) Biochemistry of DNA lesions. Radiat Res 104: S103–S111

Ward J (1990) The yield of DNA double-strand breaks produced intracellularly by ionizing radiation: a review. Int J Radiat Biol 57:1141–1150

Weber K, Flentje M (1993) Lethality of heavy ion induced DNA double-strand breaks in mammalian cells. Int J Radiat Biol 64: 169–178

Wlodek D, Hittelman W (1988) The relationship of DNA and chromosome damage to survival of synchronized x-irradiated L5178Y cells. Radiat Res 115:550–565

Wlodek D, Banáth J, Olive P (1991) Comparison between pulsed-field and constant field gel electrophoresis for measurement of DNA double-strand breaks in irradiated Chinese hamster ovary cells. Int Radiat Biol 60:779–790

Zirkle R, Tobias C (1953) Effects of ploidy and linear energy transfer on radiobiological survival curves. Arch Biochem Biophys 47:282–306